Available online at www.sciencedirect.com

SCIENCE DIRECT®

Optics Communications 234 (2004) 29–34

OPTICS COMMUNICATIONS

www.elsevier.com/locate/optcom

Influence of third-order dispersion on the temporal Talbot effect

Julien Fatome, Stéphane Pitois *, Guy Millot

Laboratoire de Physique de l'Université de Bourgogne, Unité Mixte de Recherche 5027, Centre National de la Recherche Scientifique, Faculté des Sciences Mirande, 9 Avenue Alain Savary, B.P. 47870, 21078 Dijon Cédex, France

Received 29 October 2003; received in revised form 4 February 2004; accepted 4 February 2004

Abstract

We study both theoretically and experimentally the influence of third-order dispersion on the temporal profile recovery induced by the Talbot effect of a 160 GHz periodic pulse train in a standard optical fiber.

PACS: 42.81.Dp; 42.65.Re

Keywords: Optical fiber; Talbot effect; Third-order dispersion; Pulse train generation

1. Introduction

It has been demonstrated that a periodic pulse train propagating in the dispersion regime (dispersion length $L_D \ll$ nonlinear length L_{NL}) of a dielectric medium such as an optical fiber, can recover its initial shape at some distances in the medium. This well-known phenomenon can be seen as a temporal analogue of the spatial Talbot effect and has been reported in various media such as single-mode optical fibers [1], multimode fibers [2] and even in Bose–Einstein condensates [3]. This phenomenon has been successfully applied to suppress the dispersion effects in a pulsed fiber laser by adjusting the cavity length to match a multiple of the Talbot length [4]. The temporal Talbot effect has been also extensively studied for multiplying the repetition rates of periodic pulse trains (fractional Talbot effect) [5–7]. An extension of these studies to the case of periodic pulse trains of finite duration has been carried out in [8]. However, all previous studies consider only the case when high-order dispersion terms can be neglected. In other words, to our knowledge, only second-order group-velocity dispersion was considered. This assumption is valid only when the fiber length is much shorter than the third-order dispersion length. In this work, we consider the

* Corresponding author. Tel.: +33-3-80-39-59-89; fax: +33-3-80-39-59-71.
E-mail address: spitois@u-bourgogne.fr (S. Pitois).

0030-4018/$ - see front matter © 2004 Elsevier B.V. All rights reserved.
doi:10.1016/j.optcom.2004.02.005

many cases when both the second- and the third-order dispersion effects cannot be neglected and we study both theoretically and experimentally the influence of third-order dispersion on the self-reshaping of a 160 GHz periodic pulse train in a standard optical fiber.

2. Theory

The electrical field of a linearly polarized light beam propagating in a single-mode optical fiber may be written as

$$\mathbf{E}(x,y,z,t) = \psi(x,y)\left[u(z,t)\,\mathrm{e}^{(\mathrm{i}\beta_0 z - \mathrm{i}\omega_0 t)} + \mathrm{c.c}\right], \tag{1}$$

where c.c denotes complex conjugation, $u(z,t)$ is the slowly varying amplitude of the envelope, β_0 is the propagation constant at frequency ω_0 and $\psi(x,y)$ is the transverse field distribution associated to the fundamental LP_{01} mode. By inserting this expression into the Maxwell's equations, under the usual slowly varying field envelope approximation, and neglecting nonlinear terms, one obtains the linear partial differential equation describing the light propagation through the fiber [9]

$$\frac{\partial u}{\partial z} = -\frac{\alpha}{2}u - \frac{\mathrm{i}}{2}\beta_2\frac{\partial^2 u}{\partial t^2} + \frac{1}{6}\beta_3\frac{\partial^3 u}{\partial t^3}, \tag{2}$$

where β_2 and β_3 are the second-and third-order dispersion coefficients, respectively. Hereafter, we will neglect the parameter α which represents the fiber losses. This assumption is valid since only the pulse shape is considered here and not the absolute magnitude of pulse intensity. Eq. (2) can be easily solved by use of the Fourier-transform method and the solution is given in the frequency domain by

$$\tilde{u}(\omega,z) = \tilde{u}(\omega,0)\exp\left(\mathrm{i}z\left[\frac{\beta_2}{2}\omega^2 + \frac{\beta_3}{6}\omega^3\right]\right), \tag{3}$$

where ω is the frequency detuning from the reference frequency ω_0. If we now assume a periodic initial pulse train with a temporal period of $2\pi/\Omega$, the field can be written as

$$\tilde{u}(\omega,0) = \sum_n a_n\delta(\omega - n\Omega). \tag{4}$$

By inserting this expression into Eq. (3), one finds that the field at any distance z is given by

$$\tilde{u}(\omega,z) = \sum_n a_n\exp\left(\mathrm{i}z\left[\frac{\beta_2}{2}(n\Omega)^2 + \frac{\beta_3}{6}(n\Omega)^3\right]\right)\delta(\omega - n\Omega). \tag{5}$$

Eq. (5) shows that the dispersive terms change the phase of each spectral component a_n by an amount that depends on the propagation distance z. It is clear that the field will be restored at certain distances L satisfying the following relation:

$$\left(\frac{\beta_2}{2}(n\Omega)^2 + \frac{\beta_3}{6}(n\Omega)^3\right)L = l_n 2\pi, \quad l_n \in N, \ \forall n. \tag{6}$$

Eq. (6) is satisfied for all n when both terms of the left-hand side are simultaneously multiple of 2π for $n = 1$, i.e. $(\beta_2/2)\Omega^2 L = k_2 2\pi$ and $(\beta_3/6)\Omega^3 L = k_3 2\pi$. This condition leads to the definition of two characteristic lengths

$$L_{\beta_2} = \frac{4\pi}{|\beta_2|\Omega^2} \tag{7}$$

and

$$L_{\beta_3} = \frac{12\pi}{|\beta_3|\Omega^3}. \tag{8}$$

L_{β_2} is the usual Talbot length whereas L_{β_3} is the distance at which the input pulse profile is perfectly restored in the absence of second-order group-velocity dispersion. When both the second- and the third-order dispersion terms are taken into account, the pulse train recovers its initial shape if the fiber length is a common multiple of L_{β_2} and L_{β_3}, i.e. if there exits integer numbers k_2 and k_3 such as

$$L = k_2 L_{\beta_2} = k_3 L_{\beta_3}. \tag{9}$$

In fact, the pulse train is also recovered if $L = \bar{k}_2 L_{\beta_2}/2 = \bar{k}_3 L_{\beta_3}/6$ ($\bar{k}_2, \bar{k}_3 \in N$) but with a temporal delay between the recovered and initial trains. This condition is easily obtained by noting that a temporal delay can be seen as a linear variation of the phase in the spectral domain. In order to characterize the pulse sequence recovery, we define the intercorrelation function between the initial sequence and the pulse train at some distance z as

$$I(z,\tau) = \int_{-\infty}^{\infty} |u(0,t)|^2 \times |u(z,t-\tau)|^2 \, dt, \qquad (10)$$

and a normalized recovery coefficient $R(z)$ [10]

$$R(z) = \frac{\max[I(z,\tau)]}{\max[I(0,\tau)]}, \qquad (11)$$

where $\max[I(z,\tau)]$ is the maximum of the function I for $\tau \in [-\infty + \infty]$. This coefficient is defined in such a way that $R(z) = 1$ if the pulse train is exactly recovered at the distance z. We emphasize that $R(z)$ is also equal to 1 when the pulse train is restored with a temporal delay. This property is illustrated by Fig. 1(a) which shows the recovery coefficient $R(z)$ calculated from numerical integration of Eq. (2) for $\Omega/2\pi = 160$ GHz and with parameters of a standard single-mode fiber (SMF) at $\lambda = 1550$ nm: $\beta_2 = -2.168 \times 10^{-2}$ ps^2/m ($D = 17.02$ ps/km/nm) and $\beta_3 = 1.2661 \times 10^{-4}$ ps^3/m ($S = 0.056$ ps/km/nm^2). With these parameters, one finds $L_{\beta_3} = 293$ km and $L_{\beta_2} = 575$ m. Fig. 1(a) clearly illustrates the two intrinsic periods of the systems, i.e. $L_{\beta_3}/6 = 48.8$ km and $L_{\beta_2}/2 = 287.5$ m. Fig. 1(b) is obtained for $\Omega/2\pi = 160$ GHz and with typical parameters of a dispersion-shifted fiber (DSF) at $\lambda = 1550$ nm: $\beta_2 = -5.22 \times 10^{-4}$ ps^2/m ($D = 0.41$ ps/km/nm) and $\beta_3 = 6.48 \times 10^{-5}$ ps^3/m ($S = 0.039$ ps/km/nm^2). With these parameters, one finds $L_{\beta_3} = 572$ km and $L_{\beta_2} = 23.8$ km.

It is now interesting to evaluate the dependence of the pulse train recovery upon the repetition rate. The dispersion-induced phase shift for the first harmonic ($n = 1$) at the fiber output can be written as

$$\phi_1 = \left[\frac{\beta_2}{2}\Omega^2 + \frac{\beta_3}{6}\Omega^3\right]L. \qquad (12)$$

From Eq. (12), and by considering the parameters of a standard optical fiber at $\lambda = 1550$ nm, one can easily ascertain that a deviation of 0.1 GHz of the pulse train repetition rate leads to a phase deviation of about $2\pi/10$. Such a deviation will induce severe degradations in the pulse train shape as illustrated in Fig. 2(a), which shows the pulse train intensity at the end of the fiber for $\Omega/2\pi = 160.1$, 160.01 and 160.001 GHz. The length of the fiber is $L = L_{\beta_3} = 511L_{\beta_2}$. As can be seen in Fig. 2(a), the Talbot process is very sensitive to any frequency jitter of the pulse sequence and therefore one cannot expect to observe experimentally this effect if the repetition rate of the optical pulse train is not carefully controlled. However, one can see from

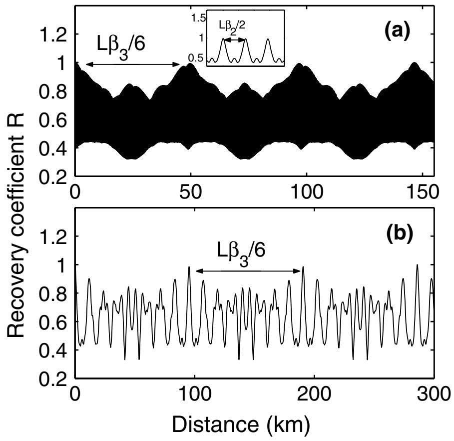

Fig. 1. Evolution of the recovery coefficient $R(z)$ with the distance. (a) $L_{\beta_3}/6 = 48.8$ km and $L_{\beta_2}/2 = 287.5$ m. The inset represents a zoom around $z = L_{\beta_3}/6$. (b) $L_{\beta_3}/6 = 95.3$ km and $L_{\beta_2}/2 = 11.9$ km.

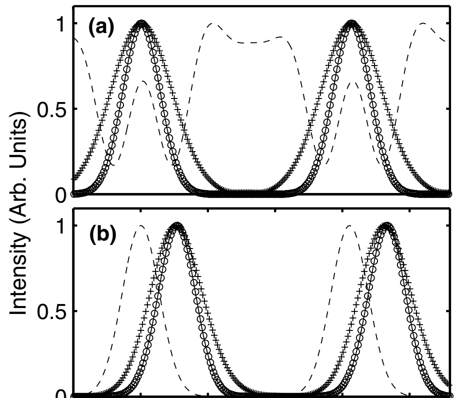

Fig. 2. (a) Pulse train at the fiber output for $\Omega = 160$ GHz (solid line), $\Omega = 160.001$ GHz (circles), $\Omega = 160.01$ GHz (crosses) and $\Omega = 160.1$ GHz (dashed line). The fiber length is $L = L_{\beta_3} = 511L_{\beta_2}$. (b) Pulse train at the fiber output for $\Omega = 160$ GHz (solid line), $\Omega = 160.1$ GHz (circles), $\Omega = 161$ GHz (crosses). Dashed line: pulse train at the fiber input. The fiber length is $L = L_{\beta_3}/6 = 4L_{\beta_2}$.

Eq. (12) that the frequency tolerance can be increased by minimizing the value of β_2 or/and by minimizing the fiber length. In practice, the group-velocity dispersion can be decreased by compensating the negative dispersion of the standard fiber with a fiber with positive dispersion. The length of the fiber can also be decreased by noting that the pulse train is also recovered if $L = L_{\beta_3}/6$ but with a temporal delay between the recovered train and the original train.

Therefore, in what follows, we consider the situation where the standard fiber with length L_1 is followed by a compensating fiber with length L_{comp}. We use β_2^{comp} and β_3^{comp} to designate the second-order and third-order group-velocity dispersion parameters of the compensating fiber, respectively. The length of the system is now $L = L_1 + L_{\mathrm{comp}}$. Here, Eq. (9) remains valid except that L_{β_2} and L_{β_3} are now defined in terms of average second-order group-velocity dispersion $\beta_2^{\mathrm{av}} = (\beta_2 L_1 + \beta_2^{\mathrm{comp}} L_{\mathrm{comp}})/(L_1 + L_{\mathrm{comp}})$ and average third-order dispersion $\beta_3^{\mathrm{av}} = (\beta_3 L_1 + \beta_3^{\mathrm{comp}} L_{\mathrm{comp}})/(L_1 + L_{\mathrm{comp}})$.

Fig. 2(b) represents the intensity of a pulse train at the output of the compensating fiber for the following parameters: $\Omega/2\pi = 160$ GHz, $L_1 \simeq 97.6$ km, $\beta_2 = -0.0217$ ps^2/m and $\beta_3 = 1.2661 \times 10^{-4}$ ps^3/m. The compensating fiber is a fiber module with the following parameters: $\beta_2^{\mathrm{comp}} L_{\mathrm{comp}} = 2.0678 \times 10^3$ ps^2 ($D^{\mathrm{comp}} L_{\mathrm{comp}} = -1622.4$ ps/nm) and $\beta_3^{\mathrm{comp}} L_{\mathrm{comp}} = -6.1537$ ps^3 ($S^{\mathrm{comp}} L_{\mathrm{comp}} = -1.695$ ps/nm^2). With these parameters, $L = 0.997 L_{\beta_3}/6 \simeq L_{\beta_3}/6$ and $L = 4L_{\beta_2}$. For convenience fiber parameters used in our numerical simulations of Fig. 2(b) correspond to those used in our experiment discussed in Section 3. We observe in Fig. 2(b), that this parameter set permits to recover the pulse train at the fiber output (solid line). The temporal delay between the original train (dashed line) and the recovered train (solid line) is equal to $T/6$, where T is the period of the pulse train. Fig. 2(b) also illustrates the pulse train at the system output for $\Omega/2\pi = 160.1$ GHz (circles) and $\Omega/2\pi = 161$ GHz (crosses). We conclude from Figs. 2(a) and (b), that the amplitude of variation of the output pulse train temporal profile as a function of the repetition rate strongly depends on the amount of dispersion. On the one hand, in case of propagation of the pulse train in a standard fiber with large second-order and third-order dispersion coefficients the output profile is very sensitive to the pulse repetition rate. On the other hand, in case of propagation in a dispersion-managed system with relatively small average values for second-order and third-order dispersion coefficients, the output profile is not as much sensitive to small variations of the pulse repetition rate, which makes the experimental observation of the Talbot effect possible. Note that a detailed discussion on tolerance with dispersion of the temporal Talbot effect in the restricted case of second-order dispersion media is given in [11].

3. Experimental results

An overview of the experimental set-up is shown in Fig. 3. The 160-GHz picosecond pulse train is generated at 1550 nm by using multiple four-wave mixing temporal compression of an initial dual frequency beat-signal propagating in a 1-km long NZ-DSF with an anomalous dispersion

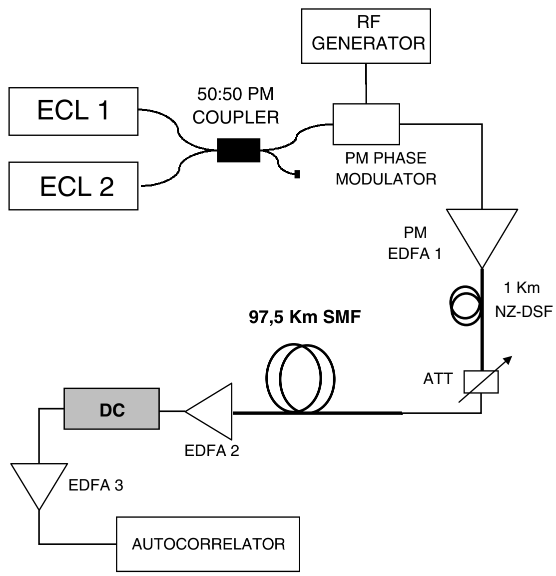

Fig. 3. Experimental set-up. ECL 1, ECL 2: external-cavity lasers; PM: polarization-maintaining; EDFA: erbium-doped fiber amplifier; ATT: variable attenuator; DC: dispersion compensator module.

of 1 ps/nm/km [12]. The beat-signal is synthesized from two cw external cavity lasers (ECLs) and amplified by an erbium-doped fiber amplifier (EDFA 1) at an average power of 27.2 dBm. A phase modulator permits to suppress the stimulated Brillouin scattering effect. After nonlinear reshaping in the NZ-DSF, 1.3-ps Gaussian pulses are generated [12]. The amplitude and phase profiles of the pulses were characterized by means of a standard FROG technique. The phase variation over the compressed pulses was found to be very small, indicating that the pulses are essentially transform-limited, with a phase difference of π between two consecutive pulses. Moreover, the extinction ratio between peak power and inter-pulse background is better than 20 dB. The pulses were then injected in $\approx$97.5 km of standard fiber (SMF) followed by a commercially available dispersion compensator made of high-order-mode fibers (HOMs). The dispersion compensator has a cumulated dispersion of 2.0678×10^3 ps^2 and a cumulated dispersion-slope of -6.1537 ps^3. After propagation through the SMF, the linear losses were exactly compensated by means of a erbium-doped fiber amplifier (EDFA 2). A variable attenuator was used to control the optical power injected into the SMF fiber. Finally, the pulse train was boosted by a EDFA (EDFA 3), before detection by a second-harmonic generation autocorrelator. The average power launched in the fiber was less than 0 dBm (1 mW) so that the total nonlinear phase ϕ_{NL} induced by the propagation can be neglected. Indeed, we have checked that $\phi_{NL} < 2\pi/100$ for the parameters used in our experiment. Finally, we point out that our theoretical developments are valid whatever the phase and amplitude profiles of the periodic pulse trains, providing that the reference frequency ω_0 coincides with a spectral band of the signal. If this condition is satisfied, the recovery condition Eq. (9) remains unchanged whatever the phase shift between adjacent initial pulses.

Fig. 4(a) shows the experimental autocorrelation traces for $\Omega/2\pi = 160$ GHz measured at the system output (circles) and input (solid line). It is clearly demonstrated in Fig. 4(a) that the temporal profile of the input pulse train is perfectly restored after propagation through the fiber line. The autocorrelation trace obtained for $\Omega/2\pi = 164$ GHz (dashed line) demonstrates that a small variation of the pulse repetition rate leads to a strong modification of the temporal profile at the system output. Indeed it is clear that, for $\Omega/2\pi = 164$ GHz, the output profile is significantly different from the initial temporal profile. The excellent agreement between the experimental results and the theoretical predictions obtained by numerical integration of Eq. (2) (see Fig 4(b)) evidences the role of the third-order dispersion on the Talbot effect.

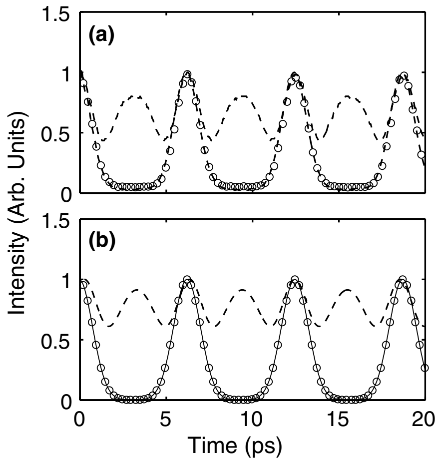

Fig. 4. (a) Plot showing the experimental autocorrelation traces of the pulse train measured at the fiber output for $\Omega = 160$ GHz (circles) and $\Omega = 164$ GHz (dashed line), in comparison with those measured at the fiber input for $\Omega = 160$ GHz (solid line). (b) Plot showing the corresponding theoretical autocorrelation traces.

4. Conclusion

In summary, we have investigated the influence of the third-order dispersion effect on the temporal Talbot effect in a standard optical fiber. In particular, we have pointed out that the recovery of the pulse train can be highly sensitive to the laser source repetition rate. This issue has been experimentally resolved by decreasing both the length and the group-velocity dispersion of the system. The measured autocorrelation traces are in excellent agreement with the theoretical predictions, thus demonstrating the recovery of a pulse train after propagation through more than 100 km of optical fiber.

Acknowledgements

We thank P. Tchofo Dinda for a careful reading of the manuscript. We gratefully acknowledge financial support of this research by the Conseil Régional de Bourgogne, the Centre National de la Recherche Scientifique and the Ministère de la Recherche et des Nouvelles Technologies. We also thanks E. Pincemin, E. Le Rouzic, S. Gosselin, and B. Cuenot from France Telecom Lannion for stimulating discussions and for providing us the standard optical fiber and the dispersion compensating module. G. Millot acknowledges financial support from the Institut Universitaire de France.

References

[1] T. Jannson, J. Jannson, J. Opt. Soc. Am. 71 (1981) 1373.
[2] V.P. Minkovich, A.N. Starodumov, V.I. Borisov, V.I. Lebedev, S.N. Perepechko, Opt. Commun. 192 (2001) 231.
[3] L. Deng, E.W. Hagley, J. Denschlag, J.E. Simsarian, M. Edwards, C.W. Clark, K. Helmerson, S.L. Rolston, W.D. Phillips, Phys. Rev. Lett. 83 (1999) 5407.
[4] B. Fischer, B. Vodonos, S. Atkins, A. Bekker, Opt. Lett. 25 (2000) 728.
[5] N.K. Berger, B. Vodonos, S. Atkins, V. Smulakovsky, A. Bekker, B. Fischer, Opt. Commun. 217 (2003) 343.
[6] D.A. Chestnut, C.J.S. de Matos, J.R. Taylor, Opt. Lett. 27 (2002) 1262.
[7] J. Azana, M.A. Muriel, Opt. Lett. 24 (1999) 1672.
[8] J. Azana, J. Opt. Soc. Am. B 20 (2003) 83.
[9] G.P. Agrawal, in: Nonlinear Fiber Optics, Academic Press, Boston, 1989.
[10] J. Azana, M.A. Muriel, Appl. Opt. 38 (1999) 6700.
[11] J. Azana, M.A. Muriel, IEEE J. Select. Top. Quantum Electron. 7 (2001) 728.
[12] S. Pitois, J. Fatome, G. Millot, Opt. Lett. 27 (2002) 1729.